Bioresource Technology Reports 24 (2023) 101663

Contents lists available at ScienceDirect

Bioresource Technology Reports

journal homepage: www.sciencedirect.com/journal/bioresource-technology-reports

Novel dragon fruit peel ash-derived solid catalyst for biodiesel production and PET waste recycling

Vanlalngaihawma Khiangte [a,b], Samson Lalhmangaihzuala [a,b], Z.T. Laldinpuii [a,b], Lal Nunnemi [a,b], Rajendra Bose Muthukumaran [b], Khiangte Vanlaldinpuia [a,*]

[a] Department of Chemistry, Pachhunga University College, Mizoram University, Aizawl 796001, Mizoram, India
[b] Department of Chemistry, Mizoram University, Tanhril, Aizawl 796004, Mizoram, India

ARTICLE INFO

Keywords:
Dragon fruit
Ash
Heterogeneous catalyst
Biodiesel
PET depolymerization

ABSTRACT

The present protocol demonstrates the development of an affordable methodology for synthesizing biodiesel and depolymerizing PET waste using dragon fruit (*Hylocereus costaricensis* or *Hylocereus polyrhizus*) peel ash derived solid catalyst. The reported catalytic process yielded 99 % biodiesel at room temperature in 5 h with 8 wt% catalyst amounts and 12 M equivalents of methanol, while requiring just 20 min of run time at an elevated temperature (65 °C). The reaction was found to be endothermic pseudo-first order reaction having activation energy of 56.36 kJ mol^{-1}. Meanwhile, PET waste was depolymerized to bis(2-hydroxyethyl) terephthalate (BHET) in 1.5 h at 190 °C with 16 equivalents of ethylene glycol and 4 wt% of the catalyst, giving 84 % of the desired monomer. The developed catalyst and the resultant products are thoroughly characterized using a variety of techniques to determine the catalyst's chemical composition and to confirm the formation of the desired products.

1. Introduction

The demand for energy worldwide has increased significantly due to the exponential growth of population and rapid industrialization. Petroleum reserves and other fossil fuels, which have been the world's primary source of energy for decades, are nearing the end of their production life and are projected to be depleted by 2050 (Basumatary et al., 2018). Furthermore, motor vehicles are one of the greatest contributors to greenhouse gases (GhG), yet they still managed to reach almost 78 million productions in 2020 alone despite the global pandemic (*Worldwide Automobile Production | Statista [WWW Document]*, 2022). As a result, the scientific world has put much effort into the search for alternative clean fuel, either as a blending component or as an immediate substitute for non-renewable energies such as natural gas, coal and petroleum (Hameed et al., 2009). In fact, the scientific community has been drawn towards the exploration of biofuels that are renewable, environmentally friendly, long-lasting, highly efficient, and economical due to factors such as increased global energy consumption, rising GhG emissions, and a continuous increase in fossil fuel depletion, as well as rapid price fluctuations (Gohain et al., 2020). Accordingly, the introduction of fuel generated from renewable feedstocks, such as biodiesel and bioethanol, has gained considerable attention and is a viable option for compression ignition engines (Sarma et al., 2008).

Biodiesel, a diesel-equivalent processed fuel, is a mixture of monoalkyl esters of fats or oils that may be synthesized using a catalyst through the transesterification of triglycerides with anhydrous alcohol, primarily methanol (Rouhany and Montgomery, 2019). This fuel is highly renewable, clean, and emits less sulfur residue as well as carcinogenic compounds during combustion. It also possesses better outstanding qualities such as higher cetane number, flash point and lubrication properties when compared to petroleum diesel (Banković-Ilić et al., 2017). In addition, biodiesel also blended well with existing petrodiesel in all possible fractions and was tailored to be compatible with the current diesel engine without the need for any significant alteration (Changmai et al., 2020a). However, despite its all known advantages, biodiesel has not been fully commercialized yet in many parts of the world due to high production costs in contrast to its competing fossil-based fuel. Major roadblocks to its economic feasibility could be realized by applying less expensive raw materials, such as inedible oils and/or waste cooking oils, and utilization of low-cost heterogeneous catalysis for its synthesis (Betiku et al., 2017). Hence, numerous methodologies have been explored in recent years by the

* Corresponding author.
E-mail address: mapuiakhiangte@gmail.com (K. Vanlaldinpuia).

https://doi.org/10.1016/j.biteb.2023.101663
Received 12 June 2023; Received in revised form 17 September 2023; Accepted 13 October 2023
Available online 21 October 2023

scientific community for the development of economically viable biodiesel production techniques, most of which involve heterogeneous catalysts (Alemu et al., 2023). Although homogeneous catalytic systems have many desirable characteristics, such as higher selectivity and efficacy, recent research and literature reviews have shown that the use of heterogeneous catalysts for biodiesel production is steadily increasing, primarily due to their simple separation method and reusability, which also encourages a lower operational charge (Zhao et al., 2023).

Meanwhile, the world has witnessed a dramatic intensification of plastic production beginning from the 1950s, almost doubling it every year since then to produce around 367 million metric tons of plastics in 2020. The overall production in 2020 marginally declined by about 0.3 % compared with the previous year, and it was attributed to the Covid pandemic's impact on the industry (*Global Plastic Production 1950–2020 | Statista [WWW Document]*, 2020). Nevertheless, the rapid accumulation of plastic waste in the surroundings on account of its extensive production and consumption is correlated with significant environmental issues, mainly due to their low rate of recycling and biodegradability. It was previously approximated that global plastic waste production reached 6300 million metric tons in 2015, only 9 % of which are recycled, and about 79 % are cast-off to landfills and oceans (Geyer et al., 2017). Therefore, it is crucial to introduce and implement an ideal method of plastic waste management as they are almost impracticable to replace with other materials. Hence, scientific circles have introduced several methodologies for their proper disposal and recycling (Khopade et al., 2023).

Currently, poly(ethylene terephthalate) or PET is one of the most produced plastic polymers and the most widely recycled plastics in the world. Its recycling is broadly classified into four categories: viz closeloop recycling, energy recovery through incineration and pyrolysis, chemical recycling and physical recycling (Soong et al., 2022). Physical process is the current primary practice, which usually results in the formation of poor-quality secondary plastics, and therefore, it is often regarded as a down-cycling process. Chemical recycling of PET involves depolymerization to its monomer and/or oligomers followed by repolymerization to yield virgin grade PET or other value-added polymers (Naderi Kalali et al., 2023). It can be performed by any of the common depolymerization routes, such as glycolysis, hydrolysis, methanolysis, aminolysis, ammonolysis and hydrogenation, among others (Al-Sabagh et al., 2016). Chiefly due to the low solubility of PET in solvents along with its high stability, the chemical recycling processes are usually carried out under extreme reaction conditions. Among the recycling techniques mentioned above, glycolysis is considered the most convenient and least capital-intensive method (Guo et al., 2018). However, the main drawback of glycolysis could be the necessity of a catalyst for the process, without which the reaction is sluggish and depolymerization could not be accomplished entirely. Hence, over the past few years, a range of catalysts, such as alkalies, zeolites, nanoparticles, metal salts, ionic liquids, and organocatalysts have been developed and studied for their efficacy in PET glycolysis (Al-Sabagh et al., 2016; Jehanno et al., 2019). Despite these developments, there is a pressing need for the development of more advanced chemical recycling techniques that offer greater versatility and profitability, as the aforementioned methods usually suffer from complex catalyst preparation processes, tedious separation and purification procedures, high environmental cost, poor selectivity and other limitations.

In the meantime, implementing biowaste-derived heterogeneous catalysts for biodiesel production and other organic transformations has gained momentum in recent years due to their undemanding preparative procedure, low cost, ease of handling and environmental friendliness (Basumatary et al., 2021a). The use of biomass materials such as waste shells, waste animal bones, musa champa plant, pomegranate peel, plantain peel, pawpaw peel, orange peel, oil palm bunches, sugar beet waste, *Sesamum indicum*, Moringa leaves, *Carica papaya* stem, cocoa pod husk, coconut husk, peel, trunk, peduncle, and stem of banana etc., has been reported to successfully cement this methodology as profitable and economically achievable (Basumatary et al., 2023; Changmai et al., 2020b; Naidu and Venkateswarlu, 2022; Oloyede et al., 2023). In this paper, we have reported for the first time, the development of a novel dragon fruit peel ash (DFPA) as a highly effective, recoverable solid catalyst for the generation of biodiesel and recycling of PET waste.

Dragon fruit (*Hylocereus costaricensis* or *Hylocereus polyrhizus*) also known as pitahaya, pitaya or strawberry pear is an ornamental fruit belonging to the family *Cactaceae*. It normally has a pink, yellow, or orange skin, and the flesh is white, hot pink, or deep purple in color, with a sweety flavor and numerous tiny black seeds. Historically, the fruit originates from Mexico and Central and South America, and it was introduced in Southeast Asian countries by the French in the early 19th century (Wichienchot et al., 2010). This highly appealing fruit is now introduced, grown, and consumed on a global scale mostly due to the various health benefits in addition to its high nutritive value (Rebecca et al., 2008). Besides its unique appearance and sweet taste, the fruit is naturally fat-free and loaded with multiple antioxidants such as betacyanin and betaxanthin. It is also rich in fiber and carbohydrates and is referred to as a good source of vitamin E, beta-carotene and lycopene (Shofinita et al., 2021; Wichienchot et al., 2010). In that context, progressive demand and large-scale consumption of fruits lead to the generation of tremendous amounts of dragon fruit peel waste. The average weight of dragon fruit procured from the local market weight around 300–450 g, and the peel accounts for ~28 % of the fruit's body mass. Evaluation of dragon fruit peel for its antimicrobial and antioxidant properties has been conducted (Et, 2017), however, aside from that, the peel has limited uses and is considered as waste, and hence, is often discarded to landfills. To the best of our knowledge, there are no scientific reports describing the catalytic utilization of waste dragon fruit peel ash. So, in extension to our recent interest in the utilization of recyclable biomass waste-derived heterogeneous catalysts for the degradation of PET bottles and C—C bond formation (Laldinpuii et al., 2021c; Laldinpuii et al., 2021a, 2021b; Lalhmangaihzuala et al., 2023, 2020), we investigated the efficacy of uncalcined dragon fruit peel ash as a solid transesterification catalyst for the synthesis of FAME (fatty acid methyl ester) at room temperature or at 65 °C (Scheme 1) and for the chemical recycling of PET waste to its monomer (Scheme 2). Due to its simple preparation technique, which does not require additional modification for its reactivity, the present catalyst could serve as a greener catalyst for the aforementioned processes.

2. Experimental

2.1. Raw material

Soybean oil and PET bottles were obtained from surrounding areas in Aizawl, Mizoram, India. PET bottles were cleaned meticulously with distilled water to eliminate any impurities present in it. It was dried and then cut into 1–2 mm square flakes. All other chemicals were obtained from Merck, India, and unless otherwise stated, they were employed without any additional purification.

2.2. Catalyst preparation

Fresh pink dragon fruit peels were collected from Aizawl and its surrounding areas. The peels were cleaned rigorously with distilled water, sliced into smaller sections, and dried in an oven at 80 °C for 12 h. After drying, 200 g of the dried peels were burnt, the ashes produced were collected and strained using 100 British standards sieve to obtain ~21 g of fresh dragon fruit peel ash (DFPA). The finely powdered DFPA was then stored at room temperature in a closed container to prevent it from contamination with moisture and impurities before its use.

2.3. Catalyst characterization

Characterization of the prepared catalyst was carried out using BET

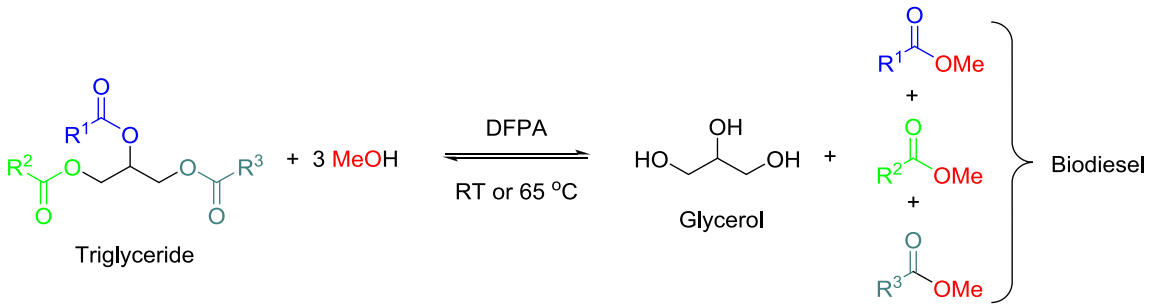

Scheme 1. Synthesis of FAME from soybean oil using DFPA

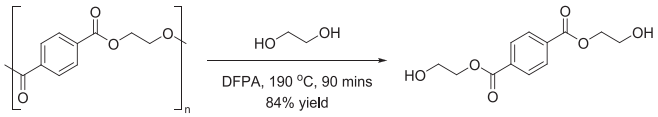

Scheme 2. Glycolysis of PET waste

(Brunauer-Emmett-Teller), TEM (Transmission Electron Microscope), SEM (Scanning Electron Microscope), XPS (X-ray Photoelectron Spectroscopy), EDX (Energy Dispersive X-ray Spectroscopy), XRF (X-ray Fluorescence), XRD (powder X-ray diffraction), FTIR (Fourier Transform Infrared Spectroscopy) and TGA (Thermogravimetric Analysis) techniques to study their pore size, morphological surface, elemental compositions, nature of crystallinity, functionality and thermal inertness. SEM and TEM images were recorded on Jeol JSM-6360 and JEM-2100, 200 kV microscope. EDX data were obtained using ESEM EDAX XL-30 instruments. For BET analysis, the sample was pre-heated at 150 °C for 4 h, and the analysis was performed with Quanta Chrome Nova-2200e. PerkinElmer TGA 4000 was used for TGA analysis and it was carried out in the range of 30–998 °C, and the sample was heated at the rate of 10 °C per minute under a nitrogen atmosphere. Philips Xpert MPD instrument was used for determining the diffraction pattern of the catalyst via XRD analysis. PerkinElmer Spectrum BX FT-IR was employed for recording FTIR data using KBr disk. XRF analysis was conducted using Rigaku ZSX Primus IV, and XPS data was recorded on ESCALAB Xi+ instrument at room temperature.

2.4. General procedure of biodiesel production

A round bottom flask (50 mL) charged with 10 g of soybean oil, 8 wt % of DFPA catalyst and 12 M equivalents of methanol was fitted with a magnetic stirrer. The reaction mixture was allowed to run at room temperature for 5 h, and thin layer chromatography (TLC) was employed to monitor the progress of the reaction. After completion of the reaction as shown by TLC, the mixture was centrifuged at 3500 rpm for 8 min, the liquid portion was decanted, and the catalyst was retrieved for reuse. The biodiesel and glycerol obtained were then isolated using a separating funnel; excess methanol present in the biodiesel was evaporated under reduced pressure. In case of incomplete conversion as shown by TLC, the yield of the reaction product was determined separately after purifying the crude product with column chromatography using ethyl acetate: n-hexane (1:40) mixture as an eluent and silica gel (60–120 mesh) as a stationary phase. Finally, the yield percentage of the FAME produced was determined by the Eq. (1) given below:

$$\text{Yield of FAME}\ (\%) = \frac{\text{Actual weight of FAME}}{\text{Initial weight of Soybean Oil}} \times 100 \quad (1)$$

The experiments were carried out in triplicate and the results are expressed as mean ± standard error of mean (SEM).

2.5. General procedure of PET glycolysis

A two-necked round bottom flask (100 mL) was equipped with a reflux condenser and thermometer and charged with 2.5 mmol of PET flakes (480 mg), 16 equivalent of ethylene glycol (EG, 2.25 mL) and 4 wt % of the prepared catalyst (DFPA, 20 mg). The reaction mixture was submerged in an oil bath pre-heated at 190 °C and allowed to run at that temperature under atmospheric pressure (Laldinpuii et al., 2021c). After the reaction was completed as shown by the total disappearance of PET granules, the reaction mixture was filtered and the residual catalyst was washed with 100 mL of hot deionized water. The filtrate was collected and allowed to cool down at room temperature, followed by vigorous stirring to dissolve all water-soluble products. It was then filtered to isolate water-insoluble oligomers from excess EG and the product. The filtrate was collected and reduced to about 30 mL, allowed to cool down and then stored at 2 °C where recrystallized bis(2-hydroxyethyl) terephthalate (BHET) separates out. The recrystallized product was isolated, dried in a hot air oven and weighed. The BHET yield percentage was calculated using Eq. (2) given below:

$$\text{BHET yield}\ (\%) = \frac{\text{Actual yield of BHET}}{\text{Theoretical yield of BHET}} \times 100 \quad (2)$$

The findings of the studies, which were carried out in triplicate, are shown as mean ± standard error of mean (SEM).

2.6. Characterization of FAME and BHET

^{1}H NMR and ^{13}C NMR data for the crude biodiesel and recrystallized BHET were recorded on Bruker, AC-400 in $CDCl_3$ and DMSO-d_6, respectively. Chemical shifts were measured in δ with tetramethyl silane (TMS) as a reference. The ^{1}H NMR spectral data of FAME was used for determining the conversion percentage of FAME using Eq. (3) (Gohain et al., 2020).

$$\text{FAME conversion}\ (\%) = \frac{2 \times I_{OCH_3}}{3 \times I_{\alpha CH_2}} \times 100 \quad (3)$$

where, I_{OCH_3} and $I_{\alpha CH_2}$ are the integral value of methoxy protons and the integral value of α-methylene protons, respectively.

Perkin Elmer Autosystem XL GC with Turbomass having capillary column PE-5 MF (0.25 mm × 30 m dimensions) and single quadrupole Mass spectrometer detector was used for GC–MS analysis. The temperature of the oven was first kept at 75 °C for 5 min, then increased to 180 °C at the rate of 10 °C/min. The oven was maintained at that temperature for 5 min, before being increased to 260 °C at the same rate. Then, the sample (2 μL) was loaded and run using helium gas as carrier which split in the ratio of 30:1 at a flow rate of 1 ml/min. The injection temperature and electron ionization temperature were maintained at 260 °C and 220 °C, respectively, and the compositions of the biodiesel were identified using TurboMass NIST 2008 software. FT-IR analysis of BHET was performed on PerkinElmer spectrum BX FT-IR instrument using KBr disks (ν_{max} in cm^{-1}) and Waters 1525 equipped with a reverse

column (Spherisorb ODS2) and Waters 2489 UV detector adjusted at 254 nm was used for HPLC (High Performance Liquid Chromatography) analysis. The density of FAME was measured using a hydrometer following the ASTM D1298 test method, while saponification number and iodine value were respectively investigated using ASTM D1962 and EN 14111 test method (Thangarasu and Anand, 2019). Kinematic viscosity of FAME was assessed using Ostwald's viscometer at 40 °C employing the ASTM D445 test technique, and the flash point and cloud point were determined according to ASTM D93 and ASTM D2500, respectively (Rupasianghe and Gunathilaka, 2018; Thangarasu and Anand, 2019). The cetane number, higher heating value, American petroleum index, diesel index and aniline point were determined using the approved standard equation of ASTM D2015 (Adepoju et al., 2018).

3. Results and discussion

3.1. Catalyst characterization

The specific composition of metallic and non-metallic oxides of DFPA was examined using XRF analysis and the result is shown in Table 1. Potassium oxide with 59.02 % was observed to be the major component followed by magnesium oxide (5.71 %), nickel oxide (4.86 %), calcium oxide (3.18 %), silicon dioxide (2.41 %), etc. in varying concentrations. The high catalytic efficacy of DFPA catalyst towards transesterification is ascribed to the high availability of strong bases such as K_2O, MgO, CaO, etc., and they are also believed to be the major active sites of the catalyst. In addition, mixed metal oxide catalysts have been found to be more effective in many organic transformations due to synergistic effect when compared with pure metal oxide (Laskar et al., 2020).

The functional group content of DFPA was determined by FT-IR analysis (see Supporting Information Fig. S1a). The resultant bands at 1365 cm^{-1}, 1041 cm^{-1} and 879 cm^{-1} were assigned to the C—O stretching and bending vibrations of carbonate (Laldinpuii et al., 2021b). The characteristic peaks at 771 cm^{-1} and 702 cm^{-1} were attributed to metal-oxygen bond stretching frequencies (Basumatary et al., 2021a), and the band at 2167 cm^{-1} was ascribed to M—O—K stretching vibration (Gohain et al., 2020). The adsorption peak observed at 2360 cm^{-1} corresponds to the stretching vibration of C—O from CO_2 adsorbed in the sample (Guo et al., 2017).

Furthermore, the N_2 adsorption-desorption analysis was conducted to examine the BET surface area, pore volume and pore diameter of the catalyst (see Supporting Information Fig. S1b and c). The N_2 adsorption-desorption isotherm (Fig. S1b) matches a characteristic type-IV isotherm with H3 hysteresis loop to some degree, specifying the mesoporosity of the catalyst (Thommes et al., 2015). The isotherm shows the formation of monolayer adsorption at low P/P^o followed by a multilayer adsorption to the pores at the intermediate pressure range. A sharp uptake at high P/P^o and the variation of the desorption path reveals the attainment of capillary condensation in the mesopores (Bardestani et al., 2019; Thommes et al., 2015). Accordingly, the pore size distribution of the prepared catalyst was determined using Barrett-Joyner-Halenda (BJH) method, and it was found to be ranging from 3.09 to 24.57 nm with an average pore diameter of 3.450 nm. In addition, the BET surface area and average pore volume were found to be 1.290 m^2/g and 0.004 cc/g, respectively, thus supporting the N_2 adsorption-desorption isotherm. The high surface area and mesoporosity of the present catalyst are believed to be pivotal in the activation of DFPA towards transesterification of triglycerides and PET polymer.

Table 1
XRF analysis of DFPA result.

Sl. no.	Chemical component	Mass %
1.	K_2O	59.02
2.	MgO	5.71
3.	NiO	4.86
4.	CaO	3.18
5.	SiO_2	2.41
6.	Cr_2O_3	0.10
7.	Al_2O_3	0.04
8.	MnO	0.03

XRD analysis was performed to investigate the crystalline composition of DFPA and the result is listed in Fig. S1d (see Supporting Information). The clear distinctive signals of K_2O (JCPDS reference file no. 77-2176 and 77-2151) and K_2CO_3 (JCPDS reference file no. 71-1466) were observed at 2θ = 25.382, 29.465, 41.148, 27.952, 39.041, 57.561, 32.092, 37.975 and 45.468. Similarly, a distinctive peak of CaO (JCPDS reference file no. 82-1691), $CaCO_3$ (JCPDS reference file no. 87-1863) and MgO (JCPDS reference file no. 65-0476) was seen at 2θ = 32.300, 37.057, 54.395, 30.328 and 43.196. In addition, SiO_2 (JCPDS reference file no. 89-8949), Cr_2O_3 (JCPDS reference file no. 84-0315), $NiCO_3$ (JCPDS reference file no. 78-0210) and KCl (JCPDS reference file no. 89-3619) phases were also observed at 2θ = 26.009, 33.878, 33.156, 28.338, 40.502, 50.144 and 58.665. From the above XRD analysis, the catalyst is found to have a mixture of metal oxides, carbonates and chlorides, in which the most intense peak corresponds to K_2O, and this is in accordance with the XRF analysis.

Thermogravimetric analysis (TGA) was carried out to examine the firmness of the synthesized DFPA at elevated temperatures (see Supporting Information Fig. S2a). The preliminary weight loss of the catalyst (about 7–13 %) between 100 °C–200 °C was ascribed to the evaporation of the adsorbed moisture content. The second weight loss seen at a higher temperature is attributed to the disintegration of carbonic material in the form of CO and CO_2. Furthermore, the XRD and XRF data were complemented by EDX analysis of the catalyst (see Supporting Information Fig. S2b) by validating the existence of potassium (42.36 %), oxygen (39.46 %), calcium (7.98 %), magnesium (4.30 %), chlorine (3.76 %), phosphorus (1.31 %), carbon (0.60 %) and sulfur (0.25 %) in DFPA (see Supporting Information, Table S1).

SEM and TEM images were captured to study the peripheral structure and particle size of the DFPA catalyst (see Supporting Information Fig. S3). The high-resolution pictures reveal a rough texture with spongy characteristics along with a large number of pores that validate the catalyst's mesoporosity with particle sizes ranging from 4 to 20 nm.

XPS investigation was also conducted to deduce the chemical composition and bonding state of DFPA catalyst, revealing the existence of Mg, Na, O, Ca, K and C on the surface of the catalyst as shown in Fig. 1. Deconvolution of the C 1s spectra of the catalyst exhibited two humps at 284.84 eV and 288.94 eV binding energies, indicating the existence of C—C of adventitious carbon and C═O of metal carbonates, respectively (Laskar et al., 2020). The peak at 530.86 eV on O 1s spectrum discloses the presence of metal oxide (Basumatary et al., 2021a), and the peaks at 295.08 eV and 292.44 eV on the deconvoluted K 2p spectrum establish the occurrence of potassium oxide and potassium carbonate, respectively (Basumatary et al., 2023). Moreover, the peaks observed at a binding energy of 346.61 eV, 350.52 eV and 1303.94 eV on the deconvoluted spectra of Ca 2p and Mg 1s also correspond to CaO, $CaCO_3$ and MgO, correspondingly (Changmai et al., 2020a). Thus, by demonstrating the presence of mixed metal oxides and carbonates in the catalyst, XPS analysis further affirms the findings of XRD, XRF, and FT-IR analyses.

3.2. Optimization for transesterification reaction

3.2.1. Optimization of catalyst amount

The impact of catalyst dosage on the conversion of oil to biodiesel was studied, and the result is illustrated in Fig. 2a. Investigations were performed at room temperature using various catalyst loading (3–10 wt %) at a fixed methanol to oil ratio (MTOR) (12:1) and reaction time (5 h). When the reaction was carried out with 3 wt% catalyst loading, only 78 % isolated yield could be obtained. Increasing the catalyst loading, on the other hand, tends to upsurge the biodiesel yield, furnishing the best result (99 %) using 8 wt% of the ash. This initial surge in biodiesel yield

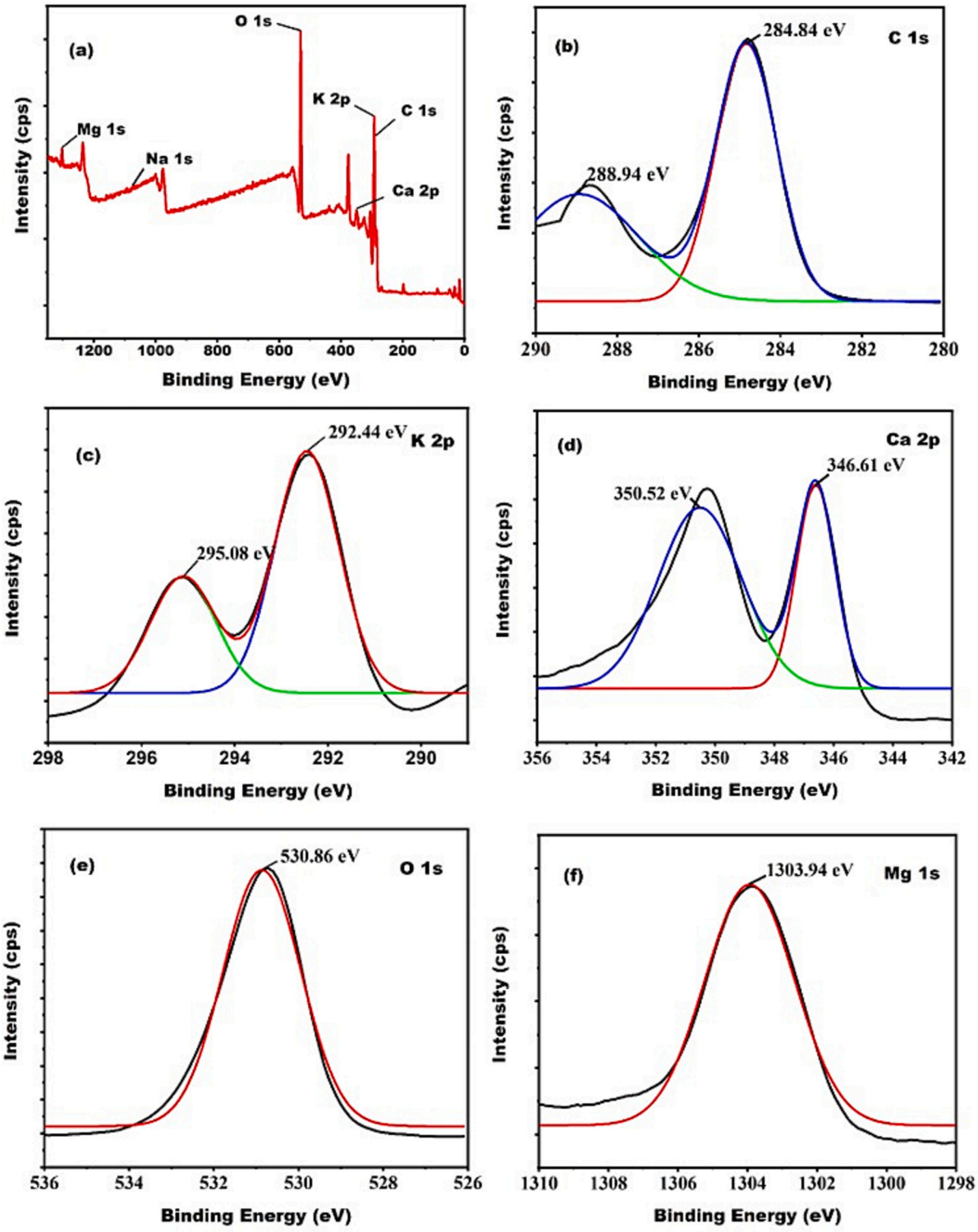

Fig. 1. (a) XPS Full survey spectrum, (b) C 1s spectra, (c) K 2p spectra, (d) Ca 2p spectra, (e) O 1s spectra, and (f) Mg 1s spectra.

with enhancing the catalyst amount is attributed to the escalation of the overall number of active sites in the reaction medium. However, a further increase in the catalyst loading beyond 8 wt% reduces the percentage yield of FAME. This might be due to the fact that the reactions loaded with a surfeit catalyst caused the mixture to become excessively viscous, preventing the catalyst from blending with the other reactants and necessitating the use of a high-powered stirrer to effectively mix the solution (Changmai et al., 2020a). The reaction mixture then attained significant overall mass transfer limitation, which subsequently decreased the conversion percentage as well as the yield of the product.

3.2.2. *Optimization of MTOR*

The methanol concentration in the reaction medium was found to have a substantial role in the effective conversion of oil into FAME (see Fig. 2b). For each successful conversion of 1 mol of oil to biodiesel, 3 mol of methanol is required (Laskar et al., 2020), and consequently, so as to enhance the forward reaction, excess methanol loading would be necessary. Thus, a series of experiments were conducted at varying

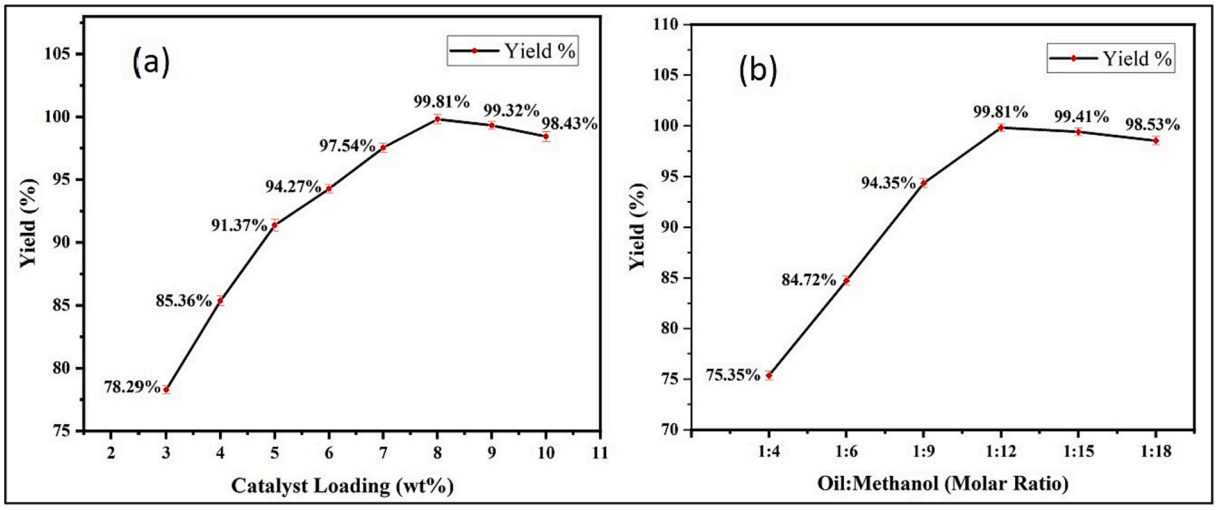

Fig. 2. (a) Influence of catalyst amount on FAME production. Reactions were conducted using 10 g of soybean oil, 12 M equivalents of methanol at room temperature for 5 h, and (b) Effect of methanol loading. Reactions were conducted using 10 g of soybean oil, 8 wt% of DFPA at room temperature for 5 h.

amounts of MTOR (4:1, 6:1, 9:1, 12:1, 15:1, 18:1) under the optimum catalyst loading (8 wt%); with a fixed reaction time of 5 h and at room temperature. Subsequently, an increase in biodiesel yield from 75 % to 85 % was seen when MTOR was enhanced from 4:1 to 6:1 M ratio. Further increase in the methanol concentration was found to have a beneficial outcome on the percentage of yield, and the highest biodiesel yield of 99 % was obtained at 12:1 MTOR. However, reactions performed with excess methanol (beyond 12:1 ratio) were observed to slightly diminish the biodiesel production, which is attributed to a decreased concentration of the catalyst in the reaction medium, which in turn decreases their effective interaction with the reactants for their efficient interaction (Laskar et al., 2018). Moreover, transesterification reaction is a reversible reaction, and employing excessive methanol has driven the reaction backward, resulting in the formation of mono and diglycerides (Pathak et al., 2018). Thus, a further increase in the methanol concentration surpassing its optimal value decreases the progress of the reaction as well as the overall biodiesel yield.

3.2.3. *Influence of reaction time*

The effects associated with reaction time on biodiesel yield were studied at the optimum condition of catalyst and methanol dosage. Experiments were conducted at varying reaction times extending from 1 to 6 h, and in each case, TLC was used to observe the progress of the reaction after every 20 min to determine the optimal reaction condition (see Fig. 3a). Initially, the product yield increases with increasing reaction time, reaching a maximum at 5 h with 99 % FAME production. However, no significant change in the production of biodiesel was observed beyond 5 h reaction time.

3.2.4. *Influence of reaction temperature*

At room temperature, the optimal condition for successful conversion of soyabean oil to FAME using DFPA catalyst was found to be 8 wt% catalyst loading, 5 h of reaction time and a 12:1 methanol to oil ratio. To further examine the possible positive impact of raising the temperature on both the reaction time as well as biodiesel yield, investigations were also performed at several reaction temperatures using the optimum condition of 12:1 MTOR and 8 wt% catalyst (see Fig. 3b). A significant reduction in reaction time from 5 h to 130 min with comparable biodiesel yield was obtained when the reaction temperature was raised from room temperature to 35 °C. At 65 °C, complete conversion was achieved within 20 min while the biodiesel yield remained unchanged. Additional increase in reaction temperature above 65 °C marginally reduces the biodiesel yield. When the reaction was performed at 75 °C, vaporization of methanol induces methanol concentration in the

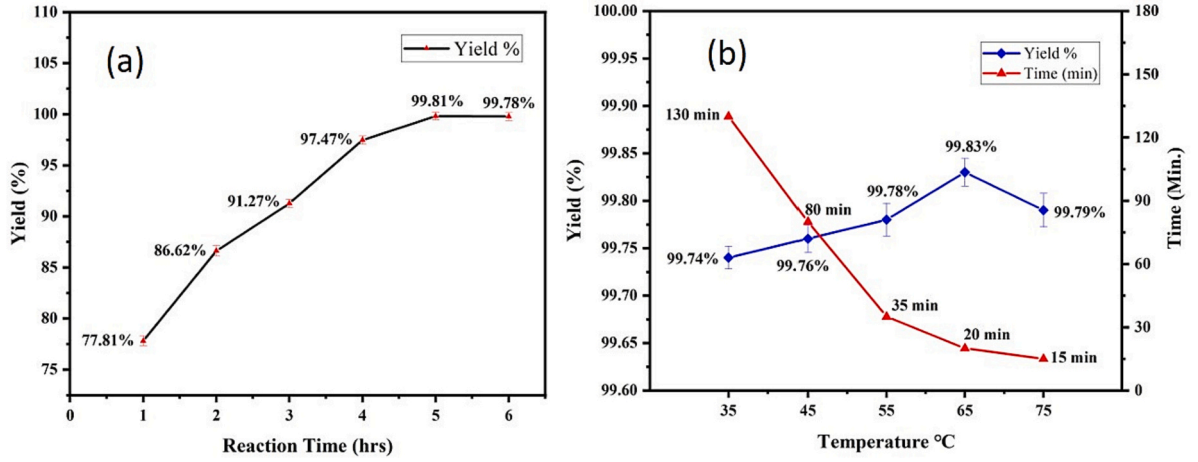

Fig. 3. (a) Influence of reaction time on biodiesel production. Reactions were conducted using 10 g of oil, 12 M equivalents of methanol, 8 wt% of DFPA at room temperature, and (b) Influence of reaction temperature on biodiesel production. Reactions were conducted using 10 g of oil, 12 M equivalents of methanol and 8 wt% of DFPA.

reaction medium to get lower, thereby causing less interaction between the oil and catalyst and hence, the decrease in biodiesel yield.

Several reactions were then performed to find the optimum catalyst loading as well as MTOR while keeping the reaction temperature constant at 65 °C (see Supporting Information, Table S2). It was observed that the amount of catalyst required for successful conversion of oil to biodiesel could be reduced to 6 wt% when the reaction was performed at elevated temperature, but at the expense of a slightly longer reaction time (30 min). When the MTOR was decreased to 9:1 (methanol:oil), reaction was completed after 2 h with 98 % biodiesel yield. From these investigations, it was concluded that even at 65 °C, the best condition for FAME production using DFPA from soybean oil is still at 8 wt% catalyst loading and 12:1 MTOR.

3.3. Reusability of the catalyst

Heterogeneous catalysis generally demonstrates easy recovery and reusability over their homogeneous counterparts, an advantage that basically minimizes the processing charge of a chemical transformation (Kumar and Ali, 2013). In that context, to explore its recyclability, DFPA catalyst retrieved from the crude reaction mass after each run via centrifugation was washed thoroughly with hexane and ethyl acetate to eliminate any unwanted residue, followed by drying in an oven at 80 °C for 4–5 h. The catalytic activity of the recycled catalyst was then investigated at 65 °C under the optimum condition of 12:1 MTOR and 8 wt% of catalyst for 7 consecutive rounds. As may be seen from Fig. 4a, the transformation of soybean oil to biodiesel slightly decreases after each successive run, reducing from 99 % in the first run to 77 % isolated yield in the seventh run. This decrease in the yield of FAME produced from oil was attributed to the leakage of the active sites to the reaction media, which eventually minimizes the catalyst's capacity to generate the same catalytic prowess after each successful conversion (Basumatary et al., 2021a).

To disclose the chemical component of the recycled catalyst, EDX analysis was performed after the 7th run, which indicates a considerable loss of K from 42.36 % to 29.02 % (see Supporting Information, Fig. S4). This slight loss of K concentration in the recovered catalyst may be the reason behind its reduced activity. In addition, the external morphology of the recovered catalyst was examined using SEM analysis (see Fig. 4b), which exhibited an agglomerated rough surface with high porosity comparable to that of the fresh catalyst.

3.4. Kinetic study of transesterification

The kinetics of FAME synthesis from soybean oil utilizing DFPA catalyst was calculated from the results obtained when the reaction was carried out at different ranges of temperatures (35 °C, 45 °C, 55 °C and 65 °C) as shown in Fig. 3b. And the rate constant of different possible orders of reaction was calculated using the following Eqs. (4)–(6) (Basumatary et al., 2021b).

$$\text{First order}: k = \frac{2.303}{t}\, log\, \frac{[SO]^{\circ}}{[FAME]} \tag{4}$$

$$\text{Pseudo}-\text{first order}: k = -\frac{2.303}{t}\, log\, \{1-[FAME]\} \tag{5}$$

$$\text{Second order}: k = \frac{2.303}{t\{[SO]^{\circ}-m\}} log \frac{m\{[SO]^{\circ}-z\}}{[SO]^{\circ}(m-z)} \tag{6}$$

where, $[SO]^{\circ}$ = Initial concentration of soybean oil; [FAME] = Concentration of biodiesel at time 't'; z = {$[SO]^{\circ}$-[FAME]} (at time 't'); m = Initial concentration of methanol based on stoichiometry {~3 × $[SO]^{\circ}$}.

$$ln k = -\left(\frac{Ea}{R}\right)\frac{1}{T} + ln A \tag{7}$$

Accordingly, plot of ln k vs 1/T was drawn using Arrhenius Eq. (7) from the calculated rate constant obtained from various reaction models (see Supporting Information Table S3) and is shown in Fig. 5a. The experimental data well supports pseudo-first order reaction with R^2 = 0.98133, while the R^2 value of first order and second order reaction comes at 0.96545 and 0.96543, respectively. This result readily confirms the theoretical assumption of pseudo-first order in which one reactant is present in excess concentration. The activation energy of 56.36 kJ mol^{-1} calculated from the slope (=−Ea/R) of Arrhenius plot lies within the reported Ea value of ~21–84 kJ mol^{-1} for the catalytic transformation of oil into FAME, denoting a chemically controlled reaction (>25 kJ mol^{-1}) (Basumatary et al., 2021a). Barros et al. and Maneerung et al. have reported a higher Ea value of 86.84 kJ mol^{-1} and 78.8 kJ mol^{-1} for the transesterification of oil to biodiesel using pineapple peel ash (de S. Barros et al., 2020) and chicken manure-derived CaO (Maneerung et al., 2016), respectively. Similarly, a higher value of 61.23 kJ mol^{-1} activation energy was also given by tucumã peel ash (Mendonça et al., 2019), while a slightly lower Ea value of 47.82 kJ mol^{-1} was described using *Mangifera indica* peel ash (Laskar et al., 2020). These data clearly

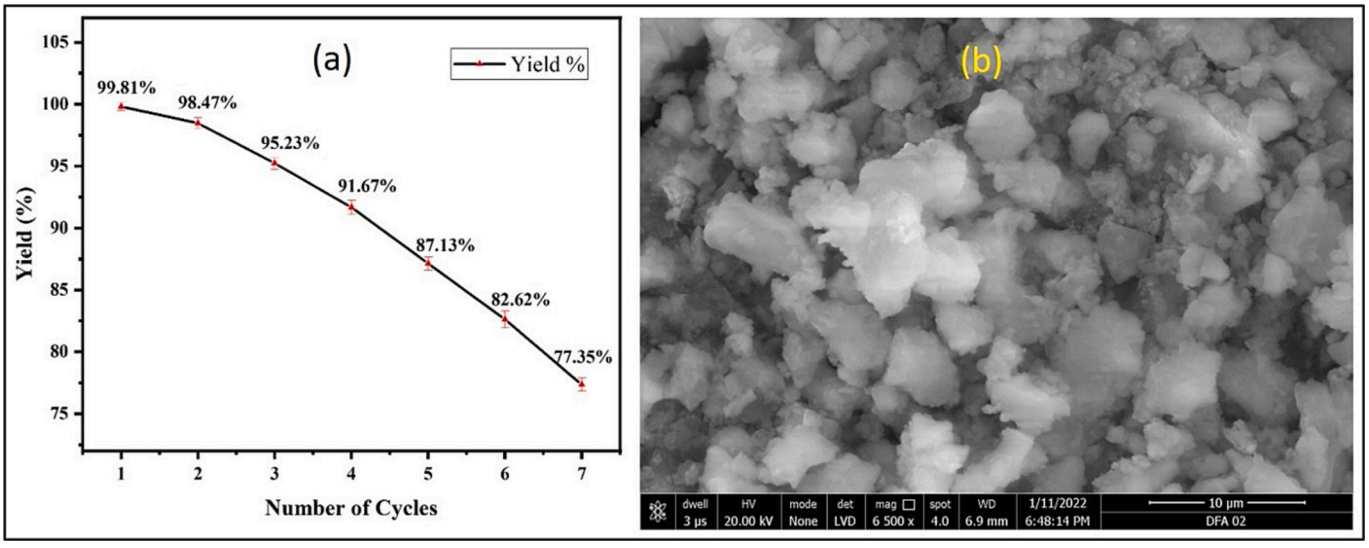

Fig. 4. (a) Reusability of the recovered DFPA catalyst. Reactions were conducted using 10 g of soybean oil, 12 M equivalents of methanol, 8 wt% DFPA at 65 °C for 20 min, and (b) SEM image of the recovered DFPA catalyst after 7th successive cycles.

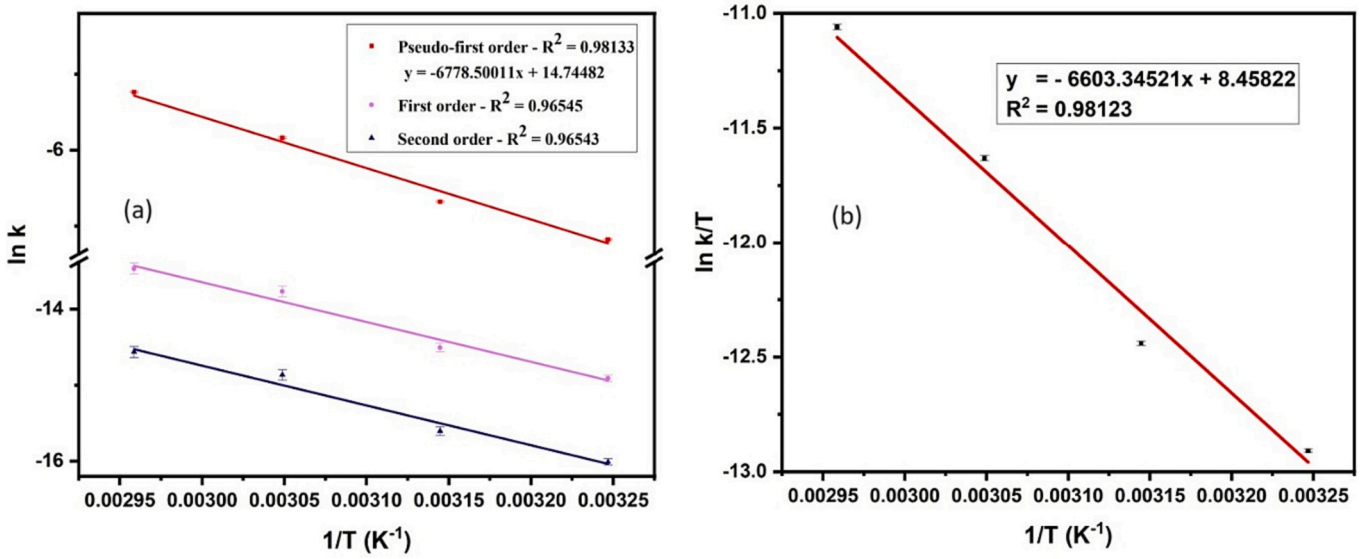

Fig. 5. (a) Arrhenius plot of different orders of reaction (ln k vs 1/T), and (b) Eyring-Polanyi plot of ln k/T vs 1/T.

indicated that DFPA catalyst could be employed for the large-scale production of biodiesel from soybean oil, substantiating its potential application at the industrial level.

3.5. Thermodynamic study of transesterification

To understand and interpret the mechanism involved in the transesterification reaction, the thermodynamic functioning of the reaction was investigated (see Supporting Information Table S4). Eyring-Polanyi Eq. (8) was employed to study the thermodynamic parameters of the reaction such as entropy change (ΔS°) and enthalpy change (ΔH°), and Gibb's free energy change (ΔG°) was calculated using Eq. (9) (Kaur and Ali, 2015). The graphical representation of ln k/T vs 1/T was plotted as shown in Fig. 5b, and the change in enthalpy (ΔH°) and entropy (ΔS°) were determined from the slope ($=-\Delta H^\circ/R$) and intercept ($=\ln(k_b/h) + \Delta S^\circ/R$) of the graph, respectively. The resultant enthalpy change shows a positive value of 54.90 kJ mol^{-1}, while the entropy change was calculated at −0.127 kJ K^{-1} mol^{-1}. The positive enthalpy change signifies that the reaction follows an endothermic route, while the negative value of the entropy change shows the reduction of randomness in the system (Banerjee et al., 2019; Kaur and Ali, 2015). Meanwhile, the Gibb's free energy change values calculated at 308, 318, 328 and 338 K were found to be 94.08 kJ mol^{-1}, 95.35 kJ mol^{-1}, 96.63 kJ mol^{-1} and 97.90 kJ mol^{-1}, respectively, indicating an endergonic and non-spontaneous nature of the reaction (Sarve et al., 2016).

$$ln\left(\frac{k}{T}\right) = -\left(\frac{\Delta H^\circ}{R}\right)\frac{1}{T} + \left[ln\left(\frac{k_b}{h}\right) + \frac{\Delta S^\circ}{R}\right] \quad (8)$$

$$\Delta G^\circ = \Delta H^\circ - T\Delta S^\circ \quad (9)$$

3.6. Characterization of FAME

The crude product obtained from the transesterification of triglyceride was analyzed using ^{1}H NMR and ^{13}C NMR to confirm the formation of the desired product. The ^{1}H NMR spectra of soybean oil and FAME are exhibited in Fig. S5a and b (see Supporting Information). The appearance of multiplets between δ 5.31–5.39 ppm and δ 4.12–4.31 ppm and a characteristic peak at δ 5.26 ppm signifies the presence of an olefinic protons (—C<u>H</u>=C<u>H</u>—) (Changmai et al., 2020a), methylene protons (—C<u>H</u>$_2$CO$_2$R) and methine proton (—C<u>H</u>CO$_2$R) of the soybean oil, respectively (Basumatary et al., 2021b). However, analysis of the final product using ^{1}H NMR exhibits the disappearance of the glyceridic protons (methylene protons and methine proton) along with the formation of a new singlet peak at δ 3.65 ppm, which corresponds to the three methoxy protons, thus, signifying the successful conversion of soybean oil into FAME (Basumatary et al., 2021b). Accordingly, the peak of α-CH$_2$ protons was detected as a triplet at δ 2.29 ppm. In its ^{13}C NMR spectra (see Supporting Information Figs. S6 and S7), the disappearance of glyceridic carbon peaks at δ 62.31 ppm and 69.12 ppm and the formation of a peak at δ 51.476 ppm which corresponds to methoxy carbon (—OCH$_3$) also confirm the generation of the biodiesel (Basumatary et al., 2021a). Finally, the conversion percentage of soybean to FAME evaluated using eq. (3) was found to be 99.98 %.

The fatty acid esters constituent of soybean oil biodiesel was investigated using GC–MS technique. The chromatogram is illustrated in Fig. S8 (see Supporting Information) and the components are listed in Table 2. Methyl linoleate, methyl palmitate, and methyl stearate were found to be the major components of FAME with 82.635 %, 10.77 %, and 6.14 % area percentage, respectively. Meanwhile, trace amounts of methyl eicosanoate (0.06 %), methyl docosanoate (0.19 %) and methyl triacontanoate (0.21 %) were also found in the synthesized biodiesel.

The various physicochemical properties of the synthesized biodiesel were evaluated employing various techniques as mentioned in the Experimental section, and the results are presented in Table 3. The density, kinematic viscosity, cetane number, flash point, saponification number (SN), iodine value, heat of combustion, etc., were all within the standards of ASTM D6751 and are comparable to other reported values for biodiesel.

3.7. Comparative analysis of DFPA with other biowaste-derived catalysts and the proposed reaction mechanism

An assessment of the catalytic activity of the DFPA with other reported biomass waste-derived heterogeneous catalysts is presented in

Table 2
GC–MS data of the crude product.

Sl. no.	R.T.	Compound name	Corresponding acid	Area %
1	20.536	Methyl palmitate	C16:0	10.77 %
2	22.536	Methyl linoleate	C18:2	82.63 %
3	22.661	Methyl stearate	C18:0	6.14 %
4	24.167	Methyl eicosanoate	C20:0	0.06 %
5	24.377	Methyl docosanoate	C22:0	0.19 %
6	26.113	Methyl triacontanoate	C30:0	0.21 %

Table 3
Physical and chemical properties of soybean oil and its biodiesel.

Properties	ASTM D6751	Soybean oil	Biodiesel
Density @15 °C	0.86–0.90	0.941	0.861
Kinematic viscosity @40 °C (mm^2/s)	1.90–6.0	34.3	5.93
Cetane number	≥47	38	51
Flash point (°C)	>93	321	146
SN (mg KOH/g)	NS	190	187
Iodine value (g I_2/100 g)	NS	129.2	107.5
HG in MJ/kg	NS	39.3	40.14
Cloud point (°C)	−3 to 12	−8	1
Aniline point	331	264.62	174.52
Diesel Index	50.4	49.94	57.32
API	36.95	18.87	32.84

SN – saponification number, HG – heat of combustion, NS – not specified.

Table S5. Several such catalysts have exhibited remarkable activity towards biodiesel production from oil, giving excellent yields with outstanding methodologies. However, in some cases, preparation of the catalyst requires calcination at high temperatures, which ultimately limits its general applicability. Apart from that, long reaction time, high MTOR and high reaction temperature are some of the limiting factors. Similar catalysts produced by burning biomass waste such as banana trunk, *Mangifera indica* peel, orange peel, wheat straw, and banana peel were shown to be comparable in efficacy, yielding up to 98.95 % biodiesel (see Supplementary Information Table S5, entries 2, 11, 15, 28, and 29). Similar to our findings, the principal components of these catalysts were oxides and carbonates of K and Ca, with the exception of wheat straw, which was found to be mostly constituted of sylvite and calcite.

From the above comprehensive analysis of the present catalyst, the oxides and carbonates of K, Ca, Mg, etc., are assumed to be the active sites that promote the synthesis of FAME from soybean oil. Hence, a plausible mechanistic pathway employing DFPA as a base catalyst is proposed and illustrated in Scheme S1 (see Supporting Information). The reaction was initiated with the removal of the proton of methanol by DFPA catalyst to form methoxide ion. The methoxide ion further attacks the electron-deficient carbon center of the ester group of triglyceride to form tetrahedral intermediate (Ullah et al., 2016), which rearranges to form methyl ester (biodiesel) and diglyceride. Conversion of the ester groups of the triglyceride to methyl ester will occur succeedingly until the generation of glycerol (Basumatary et al., 2021a).

3.8. Glycolysis of PET

As illustrated in Scheme 2, the effectiveness of the present catalyst on another transesterification reaction was explored further by performing glycolysis of PET waste to BHET monomer. Reactions were conducted in a round bottom flask charged with PET flakes, EG and DFPA at a temperature of 190 °C. In each case, the gradual disappearance of PET granules was seen as a signal for the advancement of the reactions. After the end of each reaction, the crude as well as the recrystallized products were isolated and subjected to various chemical analyses to confirm the production of the desired product.

Investigation of the crude product by means of HPLC revealed three distinctive signals at a retention time of 6.364 (BHET dimer), 3.385 (BHET monomer) and 1.856 (ethylene glycol) min (see Supporting Information Fig. S9a). This HPLC data was consistent with our previously reported data and validated with commercially available compounds (Lalhmangaihzuala et al., 2020). A sharp characteristic peak observed at 1265 cm^{-1} in its FT-IR spectra is allotted to the C—O bond stretching in ester. Absorption bands at $\nu = 3278$, 2954 and 1712 cm^{-1} designated the existence of hydroxy, methyl and carbonyl groups, correspondingly (see Supporting Information Fig. S10).

^{1}H NMR analysis of the recrystallized product (see Supporting Information Fig. S9b) discloses chemical shift values at $\delta = 8.124$ ppm (Ar—H), 4.941 ppm (O—H), 4.32 ppm (COO—CH_2—) and 3.72 ppm (CH_2—OH) and its ^{13}C NMR (see Supporting Information Fig. S11) resonates at $\delta = 165.11$ (carbonyl carbon), 133.71 and 129.46 ppm (aromatic carbons), 66.97 ppm (—O—CH_2—CH_2—OH) and 58.94 ppm (—O—CH_2—CH_2—OH), which further confirmed the generation of the desired monomer (Lalhmangaihzuala et al., 2023). Different reaction parameters were then examined to achieve the optimal condition for PET waste recycling using DFPA.

The effect of the catalyst amount in catalyzing the glycolysis of PET waste is presented in Table 4. In the absence of the present catalyst, no glycolysis occurs even after 5 h of reaction time. However, addition of just 1 wt% of DFPA results in the formation of BHET monomer in 71 % yield. The yield of BHET increases gradually with a further increase in the catalyst's concentration, and a maximal value was reached when the concentration of DFPA is at 4 % by weight. An additional increase in the catalyst loading beyond 4 wt% was found to have no major impact on the reaction; rather, a slight decrease in the yield of BHET was detected, which was accompanied by an augmented formation of a water-insoluble part. This is possibly due to the repolymerization of BHET monomer to its oligomers (Al-Sabagh et al., 2016).

The temperature of the reaction was found to have played an important role in the depolymerization of PET polyester. Glycolysis of PET is an endothermic reaction and is usually carried out in the range of 180–300 °C even in the presence of catalysts (Schaerer et al., 2022). Moreover, BHET monomer formation favors elevated temperature and so, several reactions were performed at a temperature range between 150 and 200 °C to study the influence of temperature on the glycolysis and the result is shown in Table S6 (see Supporting Information). At 150 °C, the reaction took 53 h to complete suggesting that total depolymerization could be accomplished even at a relatively lower temperature with our catalyst. With a rise in the reaction temperature, the BHET yield also increases with a significant reduction in the reaction time. The maximum yield of the desired monomer was attained at 190 °C with a maximum reaction time of 1.5 h. Further increase in the reaction temperature beyond the optimal condition results in the decreased production of BHET along with an increased formation of oligomers.

The influence of reaction time on the glycolytic depolymerization of PET is shown in Table S7 (see Supporting Information). Since glycolysis is a reversible process, identifying the optimal time at which the equilibrium between BHET dimer and monomer is reached is crucial as it could result in the maximum production of the desired product. Hence, investigations were conducted at different time intervals to determine the equilibrium point between BHET monomer and dimer. All the PET flakes disappeared even after just 30 min of reaction time, indicating the complete depolymerization of the polyester. However, the best yield of the product was achieved after 1.5 h of reaction time. Shorter or longer reaction time other than this optimal condition causes the increased generation of water-insoluble product, which reveals that the equilibrium point is reached after a reaction time of 1.5 h with DFPA catalyst.

The amount of ethylene glycol present in the reaction mixture was

Table 4
Effect of catalyst concentration.

Sl no.	Catalyst amount (in wt%)	Time (in h)	[a]BHET yield %
1	–	5	0
2	–	24	2
3	1.04	1.5	71 ± 0.83
4	2.08	1.5	78 ± 0.88
5	4.17	1.5	84 ± 0.82
6	6.25	1.5	80 ± 0.96
7	8.33	1.5	77 ± 0.88
8	10.42	1.5	75 ± 0.83

Reactions were performed with 480 mg of PET (2.5 mmol), 2.25 mL (16 eq) of EG at 190 °C.
[a] Mean ± SEM.

also found to have a great influence on both the yield as well as selectivity of the BHET monomer. Glycolysis of PET is believed to occur through diffusion of EG into PET surface in which EG both acts as reactants and reaction media (Najafi-Shoa et al., 2021). Hence, excess amount of EG must be needed to increase diffusion as well as efficient progression of the reaction. Therefore, while keeping other parameters constant at their optimum condition, PET glycolysis was carried out with an EG loading between 6 and 18 equivalents and the results are illustrated in Table S8 (see Supporting Information). The BHET yield and selectivity increase exponentially with raising in EG concentration, reaching a maximum at 16 equivalents. Lower concentration of EG is generally associated with complications in the purification and isolation procedures since the recrystallized product is consistently contaminated with a minor amount of BHET dimer and oligomers (Laldinpuii et al., 2021c; Lalhmangaihzuala et al., 2020). However, a further increase in EG loading above 16 equivalents does not improve the glycolysis process and the BHET yield, which is probably on account of the reduced concentration of the active sites of DFPA in the reaction medium.

As reported earlier in our previous works and other literature data, glycolysis of PET to BHET is believed to proceed through a stepwise reaction in which, under the influence of DFPA catalyst, the polymer first gets fragmented to form oligomers, which subsequently degenerated to form a dimer and ultimately into the monomer (George and Kurian, 2014; Laldinpuii et al., 2021c). The presence of certain metals, such as the carbonates and oxides of K, Ca and Mg in DFPA are believed to be the active sites of the transesterification process and the Lewis acid-base synergistic effect is largely credited to promoting the transformation (Laldinpuii et al., 2021c; Laldinpuii et al., 2021a, 2021b; Lalhmangaihzuala et al., 2020). Based on all this knowledge along with the above experimental results, a possible reaction mechanism was proposed and is shown in Scheme S2 (see Supporting Information). The metal cations present in the catalyst act as Lewis acid and protonate the carbonyl oxygen of the esters functionality, which causes the electrophilicity around the carbonyl carbon to increase. Meanwhile, the anionic sites in the catalyst pull protons from the ethylene glycol towards itself, generating a high electron density around the oxygen atom of the ethylene glycol. The electron-rich oxygen atoms of ethylene glycol then facilitate a nucleophilic attack on both sides of the electron-deficient carbonyl carbon of the terephthalate ester, breaking the ester linkages and resulting in the formation of new C—O bonds. As stated earlier, glycolysis is a reversible process and BHET repolymerized back to form its dimer and oligomers when the reaction progresses further.

Colored PET bottles were also depolymerized using the present catalyst to study its efficacy towards added color. These added colors usually contained acidic components (Fukushima et al., 2011) and they could hamper the transesterification process as it is a base-catalyzed reaction. Nevertheless, glycolysis of light-yellow, green and red-colored PET bottles proceeded effortlessly, giving almost comparable yield to those obtained from colorless PET under the optimized condition (see Supporting Information Table S9). Most of the pigments were removed during the filtration and recrystallization process, and any residual color, if persistent, could be eliminated by the addition of activated charcoal during the filtration process (Laldinpuii et al., 2021b).

The recyclability of the DFPA was also investigated and is summarized in Table S10 (see Supporting Information). After filtration and repeated washing with water and ethyl acetate, the recovered catalyst was dried at 80 °C for 8 h and then reused for the next five successive cycles. After each cycle, a weight loss of the catalyst by about 3–5 % is experienced which is recompensed with a fresh catalyst without any further functionalization. The second run ended with an 80 % yield of BHET monomer and a reaction time of 3 h. It was observed that after each run, there is a steady escalation in reaction time along with a decrease in the yield of BHET. This gradual loss of the catalyst's effectiveness after each cycle is attributed to the leakage of the catalyst's active sites through the filtration and purification process (Pathak et al., 2018).

4. Conclusion

This work demonstrated the successful implementation of DFPA as a catalyst for converting soybean oil to biodiesel and PET waste to BHET monomer. The transesterification reaction could be completed with 8 wt % of the catalyst at room temperature, giving the biodiesel in 99 % yield after 5 h of reaction time. At 65 °C, the reaction took only 20 min to complete, furnishing similar yield and efficacy of the procedure and the catalyst could be recycled and reused for up to 7 consecutive cycles. The same catalyst shows high catalytic effectiveness in the glycolysis of PET waste and a BHET monomer yield of 84 % could be achieved with only 4 wt% catalyst loading at 190 °C within 90 min of reaction time. The cost-effectiveness, greener methodology and easy preparation procedure of the catalyst are some of the highlights of this process.

Funding

Financial support is provided by Science and Engineering Board (SERB), New Delhi, India (File no. CRG/2022/000821 and EEQ/2017/000505).

CRediT authorship contribution statement

Vanlalngaihawma Khiangte: Formal analysis, Investigation, Data curation, Writing - original draft. **Samson Lalhmangaihzuala:** Writing - original draft, Data curation, Validation. **ZT Laldinpuii:** Formal analysis, Investigation, Writing - review and editing. **Lal Nunnemi:** Investigation, Writing - review and editing. **Rajendra Bose Muthukumaran:** Supervision, Writing - review and editing. **Khiangte Vanlaldinpuia:** Resources, Fund acquisition, Conceptualization, Methodology, Supervision, Writing - review and editing.

Declaration of competing interest

The authors declare the following financial interests/personal relationships which may be considered as potential competing interests: Khiangte Vanlaldinpuia reports financial support was provided by Science and Engineering Research Board.

Data availability

Data will be made available on request.

Acknowledgements

The authors gratefully acknowledge SICART, Gujarat, BIT, Bangalore, IIT-ISM, Jharkhand, IISc, Bangalore and CSIR-NEIST, Jorhat for sample analysis.

Appendix A. Supplementary data

Supplementary data to this article can be found online at https://doi.org/10.1016/j.biteb.2023.101663.

References

Adepoju, T.F., Olatunbosun, B.E., Olatunji, O.M., Ibeh, M.A., 2018. Brette Pearl Spar Mable (BPSM): a potential recoverable catalyst as a renewable source of biodiesel from Thevetia peruviana seed oil for the benefit of sustainable development in West Africa. Energy Sustain Soc 8, 1–17. https://doi.org/10.1186/S13705-018-0164-1/TABLES/16.

Alemu, T., Alemu, A.G., Alemu, T., Alemu, A.G., 2023. Recent developments in catalysts for biodiesel production applications. In: Advanced Biodiesel - Technological Advances, Challenges, and Sustainability Considerations [Working Title]. https://doi.org/10.5772/INTECHOPEN.109483.

Al-Sabagh, A.M., Yehia, F.Z., Eshaq, G., Rabie, A.M., ElMetwally, A.E., 2016. Greener routes for recycling of polyethylene terephthalate. Egypt. J. Pet. 25, 53–64. https://doi.org/10.1016/J.EJPE.2015.03.001.

Banerjee, S., Sahani, S., Chandra Sharma, Y., 2019. Process dynamic investigations and emission analyses of biodiesel produced using Sr–Ce mixed metal oxide heterogeneous catalyst. J. Environ. Manage. 248, 109218 https://doi.org/10.1016/J.JENVMAN.2019.06.119.

Banković-Ilić, I.B., Miladinović, M.R., Stamenković, O.S., Veljković, V.B., 2017. Application of nano CaO–based catalysts in biodiesel synthesis. Renew. Sustain. Energy Rev. 72, 746–760. https://doi.org/10.1016/j.rser.2017.01.076.

Bardestani, R., Patience, G.S., Kaliaguine, S., 2019. Experimental methods in chemical engineering: specific surface area and pore size distribution measurements—BET, BJH, and DFT. Can. J. Chem. Eng. 97, 2781–2791. https://doi.org/10.1002/CJCE.23632.

Basumatary, S., Nath, B., Kalita, P., 2018. Application of agro-waste derived materials as heterogeneous base catalysts for biodiesel synthesis. J. Renew. Sustain. Energy 10, 043105. https://doi.org/10.1063/1.5043328.

Basumatary, B., Basumatary, S., Das, B., Nath, B., Kalita, P., 2021a. Waste Musa paradisiaca plant: an efficient heterogeneous base catalyst for fast production of biodiesel. J. Clean. Prod. 305, 127089 https://doi.org/10.1016/J.JCLEPRO.2021.127089.

Basumatary, B., Das, B., Nath, B., Basumatary, S., 2021b. Synthesis and characterization of heterogeneous catalyst from sugarcane bagasse: production of jatropha seed oil methyl esters. Curr. Res. Green Sustain. Chem. 4 https://doi.org/10.1016/J.CRGSC.2021.100082.

Basumatary, B., Brahma, S., Nath, B., Basumatary, S.F., Das, B., Basumatary, S., 2023. Post-harvest waste to value-added materials: Musa champa plant as renewable and highly effective base catalyst for Jatropha curcas oil-based biodiesel production. Bioresour. Technol. Rep. 21, 101338 https://doi.org/10.1016/J.BITEB.2023.101338.

Betiku, E., Etim, A.O., Pereao, O., Ojumu, T.V., 2017. Two-step conversion of neem (Azadirachta indica) seed oil into fatty methyl esters using a heterogeneous biomass-based catalyst: an example of cocoa pod husk. Energy Fuels 31, 6182–6193. https://doi.org/10.1021/acs.energyfuels.7b00604.

Changmai, B., Sudarsanam, P., Rokhum, L., 2020a. Biodiesel production using a renewable mesoporous solid catalyst. Ind. Crop. Prod. 145 https://doi.org/10.1016/j.indcrop.2019.111911.

Changmai, B., Vanlalveni, C., Ingle, A.P., Bhagat, R., Rokhum, L., 2020b. Widely used catalysts in biodiesel production: a review. RSC Adv. 10, 41625–41679. https://doi.org/10.1039/D0RA07931F.

de S. Barros, S., Pessoa Junior, W.A.G., Sá, I.S.C., Takeno, M.L., Nobre, F.X., Pinheiro, W., Manzato, L., Iglauer, S., de Freitas, F.A., 2020. Pineapple (Ananás comosus) leaves ash as a solid base catalyst for biodiesel synthesis. Bioresour. Technol. 312 https://doi.org/10.1016/j.biortech.2020.123569.

Et, M., 2017. Effectiveness of the red dragon fruit (Hylocereus polyrhizus) peel extract as the colorant, antioxidant, and antimicrobial on beef sausage. MANIHURUK ET AL./Media Peternakan 40, 47–54. https://doi.org/10.5398/medpet.2017.40.1.47.

Fukushima, K., Coulembier, O., Lecuyer, J.M., Almegren, H.A., Alabdulrahman, A.M., Alsewailem, F.D., McNeil, M.A., Dubois, P., Waymouth, R.M., Horn, H.W., Rice, J.E., Hedrick, J.L., 2011. Organocatalytic depolymerization of poly(ethylene terephthalate). J. Polym. Sci. A Polym. Chem. 49, 1273–1281. https://doi.org/10.1002/POLA.24551.

George, N., Kurian, T., 2014. Recent developments in the chemical recycling of postconsumer poly(ethylene terephthalate) waste. Ind. Eng. Chem. Res. 53, 14185–14198. https://doi.org/10.1021/IE501995M.

Geyer, R., Jambeck, J.R., Law, K.L., 2017. Production, use, and fate of all plastics ever made. Sci. Adv. 3, e1700782 https://doi.org/10.1126/sciadv.1700782.

Global Plastic Production 1950–2020 | Statista [WWW Document]. URL. https://www.statista.com/statistics/282732/global-production-of-plastics-since-1950/.

Gohain, M., Laskar, K., Paul, A.K., Daimary, N., Maharana, M., Goswami, I.K., Hazarika, A., Bora, U., Deka, D., 2020. *Carica papaya* stem: a source of versatile heterogeneous catalyst for biodiesel production and C–C bond formation. Renew. Energy 147, 541–555. https://doi.org/10.1016/j.renene.2019.09.016.

Guo, X., Shi, H., Wei, X., 2017. Pore properties, inner chemical environment, and microstructure of nano-modified CFA-WBP (class C fly ash-waste brick powder) based geopolymers. Cem. Concr. Compos. 79, 53–61. https://doi.org/10.1016/J.CEMCONCOMP.2017.01.007.

Guo, Z., Lindqvist, K., de la Motte, H., 2018. An efficient recycling process of glycolysis of PET in the presence of a sustainable nanocatalyst. J. Appl. Polym. Sci. 135, 46285. https://doi.org/10.1002/APP.46285.

Hameed, B.H., Goh, C.S., Chin, L.H., 2009. Process optimization for methyl ester production from waste cooking oil using activated carbon supported potassium fl uoride. Fuel Process. Technol. 90, 1532–1537. https://doi.org/10.1016/j.fuproc.2009.07.018.

Jehanno, C., Pérez-Madrigal, M.M., Demarteau, J., Sardon, H., Dove, A.P., 2019. Organocatalysis for depolymerisation. Polym. Chem. 10, 172–186. https://doi.org/10.1039/C8PY01284A.

Kaur, N., Ali, A., 2015. Biodiesel production via ethanolysis of jatropha oil using molybdenum impregnated calcium oxide as solid catalyst. RSC Adv. 5, 13285–13295. https://doi.org/10.1039/C4RA14786C.

Khopade, K.V., Chikkali, S.H., Barsu, N., 2023. Metal-catalyzed Plastic Depolymerization. https://doi.org/10.1016/j.xcrp.2023.101341.

Kumar, D., Ali, A., 2013. Transesterification of low-quality triglycerides over a Zn/CaO heterogeneous catalyst: kinetics and reusability studies. Energy Fuels 27, 3758–3768. https://doi.org/10.1021/EF400594T/SUPPL_FILE/EF400594T_SI_001.PDF.

Laldinpuii, Z.T., Khiangte, V., Lalhmangaihzuala, S., Lalmuanpuia, C., Pachuau, Z., Lalhriatpuia, C., Vanlaldinpuia, K., 2021a. Methanolysis of PET waste using heterogeneous catalyst of bio-waste origin. J. Polym. Environ. 2021, 1–15. https://doi.org/10.1007/S10924-021-02305-0.

Laldinpuii, Z.T., Lalmuanpuia, C., Lalhmangaihzuala, S., Khiangte, V., Pachuau, Z., Vanlaldinpuia, K., 2021b. Biomass waste-derived recyclable heterogeneous catalyst for aqueous aldol reaction and depolymerization of PET waste. New J. Chem. 45, 19542–19552. https://doi.org/10.1039/D1NJ03225A.

Laldinpuii, Z., Lalhmangaihzuala, S., Pachuau, Z., Vanlaldinpuia, K., 2021c. Depolymerization of poly (ethylene terephthalate) waste with biomass-waste derived recyclable heterogeneous catalyst. Waste Manag. 126, 1–10. https://doi.org/10.1016/j.wasman.2021.02.056.

Lalhmangaihzuala, S., Laldinpuii, Z., Lalmuanpuia, C., Vanlaldinpuia, K., 2020. Glycolysis of poly(ethylene terephthalate) using biomass-waste derived recyclable heterogeneous catalyst. Polymers (Basel) 13, 37. https://doi.org/10.3390/polym13010037.

Lalhmangaihzuala, S., Laldinpuii, Z.T., Khiangte, V., Lallawmzuali, G., Thanhmingliana, Vanlaldinpuia, K., 2023. Orange peel ash coated Fe3O4 nanoparticles as a magnetically retrievable catalyst for glycolysis and methanolysis of PET waste. Adv. Powder Technol. 34, 104076 https://doi.org/10.1016/J.APT.2023.104076.

Laskar, I.B., Rajkumari, K., Gupta, R., Chatterjee, S., Paul, B., Rokhum, L., 2018. Waste snail shell derived heterogeneous catalyst for biodiesel production by the transesterification of soybean oil. RSC Adv. 8, 20131–20142. https://doi.org/10.1039/C8RA02397B.

Laskar, I.B., Gupta, R., Chatterjee, S., Vanlalveni, C., Rokhum, L., 2020. Taming waste: waste Mangifera indica peel as a sustainable catalyst for biodiesel production at room temperature. Renew. Energy 161, 207–220. https://doi.org/10.1016/J.RENENE.2020.07.061.

Maneerung, T., Kawi, S., Dai, Y., Wang, C.H., 2016. Sustainable biodiesel production via transesterification of waste cooking oil by using CaO catalysts prepared from chicken manure. Energ. Conver. Manage. 123, 487–497. https://doi.org/10.1016/J.ENCONMAN.2016.06.071.

Mendonça, I.M., Paes, O.A.R.L., Maia, P.J.S., Souza, M.P., Almeida, R.A., Silva, C.C., Duvoisin, S., de Freitas, F.A., 2019. New heterogeneous catalyst for biodiesel production from waste tucumã peels (Astrocaryum aculeatum Meyer): parameters optimization study. Renew. Energy 130, 103–110. https://doi.org/10.1016/j.renene.2018.06.059.

Naderi Kalali, E., Lotfian, S., Entezar Shabestari, M., Khayatzadeh, S., Zhao, C., Yazdani Nezhad, H., 2023. A critical review of the current progress of plastic waste recycling technology in structural materials. Curr. Opin. Green Sustain. Chem. 40, 100763 https://doi.org/10.1016/J.COGSC.2023.100763.

Naidu, B.R., Venkateswarlu, K., 2022. Dried water extract of pomegranate peel ash (DWEPA) as novel and biorenewable heterogeneous catalyst for biodiesel production and biopotent quinoxalines synthesis. Bioresour. Technol. Rep. 18, 101107 https://doi.org/10.1016/J.BITEB.2022.101107.

Najafi-Shoa, S., Barikani, M., Ehsani, M., Ghaffari, M., 2021. Cobalt-based ionic liquid grafted on graphene as a heterogeneous catalyst for poly (ethylene terephthalate) glycolysis. Polym. Degrad. Stab. 192, 109691 https://doi.org/10.1016/J.POLYMDEGRADSTAB.2021.109691.

Oloyede, C.T., Jekayinfa, S.O., Alade, A.O., Ogunkunle, O., Otung, N.A.U., Laseinde, O. T., 2023. Exploration of agricultural residue ash as a solid green heterogeneous base catalyst for biodiesel production. Eng. Rep. 5, e12585 https://doi.org/10.1002/ENG2.12585.

Pathak, G., Das, D., Rajkumari, K., Rokhum, L., 2018. Exploiting waste: towards a sustainable production of biodiesel using Musa acuminata peel ash as a heterogeneous catalyst. Green Chem. 20, 2365–2373. https://doi.org/10.1039/C8GC00071A.

Rebecca, O.P.S., Zuliara, R., Boyce, A.N., Chandran, S., 2008. Determining pigment extraction efficiency and pigment stability of dragon fruit (Hylocereus polyrhizus). J. Biol. Sci. 8, 1174–1180. https://doi.org/10.3923/JBS.2008.1174.1180.

Rouhany, M., Montgomery, H., 2019. Global Biodiesel Production: The State of the Art and Impact on Climate Change, pp. 1–14. https://doi.org/10.1007/978-3-030-00985-4_1.

Rupasianghe, C.P., Gunathilaka, K.S.S., 2018. Disaster Risk Reduction through biodiesel from yellow oleander (Thevetia peruviana). Proc. Eng. 212, 591–597. https://doi.org/10.1016/J.PROENG.2018.01.076.

Sarma, A., Sarmah, J., Barbora, L., Kalita, P., Chatterjee, S., Mahanta, P., Goswami, P., 2008. Recent inventions in biodiesel production and processing- a review. Recent Patents Eng. 2, 47–58. https://doi.org/10.2174/187221208783478552.

Sarve, A.N., Varma, M.N., Sonawane, S.S., 2016. Ultrasound assisted two-stage biodiesel synthesis from non-edible Schleichera triguga oil using heterogeneous catalyst: kinetics and thermodynamic analysis. Ultrason. Sonochem. 29, 288–298. https://doi.org/10.1016/J.ULTSONCH.2015.09.016.

Schaerer, L.G., Wu, R., Putman, L.I., Pearce, J.M., Lu, T., Shonnard, D.R., Ong, R.G., Techtmann, S.M., 2022. Killing two birds with one stone: chemical and biological upcycling of polyethylene terephthalate plastics into food. Trends Biotechnol. https://doi.org/10.1016/J.TIBTECH.2022.06.012.

Shofinita, D., Bindar, Y., Samadhi, T.W., Choliq, N.S., Jaelawijaya, A.A., 2021. Increasing the yield of powder and bioactive materials during extraction and spray drying of dragon fruit skin extracts. J. Eng. Technol. Sci. 53, 210612. https://doi.org/10.5614/J.ENG.TECHNOL.SCI.2021.53.6.12.

Soong, Y.H.V., Sobkowicz, M.J., Xie, D., 2022. Recent advances in biological recycling of polyethylene terephthalate (PET) plastic wastes. Bioengineering 9, 98. https://doi.org/10.3390/BIOENGINEERING9030098, 2022.

Thangarasu, V., Anand, R., 2019. Physicochemical fuel properties and tribological behavior of aegle marmelos correa biodiesel. In: Advances in Eco-Fuels for a

Sustainable Environment, pp. 309–336. https://doi.org/10.1016/B978-0-08-102728-8.00011-5.
Thommes, M., Kaneko, K., Neimark, A.V., Olivier, J.P., Rodriguez-Reinoso, F., Rouquerol, J., Sing, K.S.W., 2015. Physisorption of gases, with special reference to the evaluation of surface area and pore size distribution (IUPAC technical report). Pure Appl. Chem. 87, 1051–1069. https://doi.org/10.1515/PAC-2014-1117.
Ullah, F., Dong, L., Bano, A., Peng, Q., Huang, J., 2016. Current advances in catalysis toward sustainable biodiesel production. J. Energy Inst. 89, 282–292. https://doi.org/10.1016/J.JOEI.2015.01.018.
Wichienchot, S., Jatupornpipat, M., Rastall, R.A., 2010. Oligosaccharides of pitaya (dragon fruit) flesh and their prebiotic properties. Food Chem. 120, 850–857. https://doi.org/10.1016/J.FOODCHEM.2009.11.026.
Worldwide Automobile Production | Statista [WWW Document]. URL. https://www.statista.com/statistics/262747/worldwide-automobile-production-since-2000/ (accessed 1.11.23).
Zhao, C., Chen, H., Wu, X., Shan, R., 2023. Exploiting the waste biomass of durian shell as a heterogeneous catalyst for biodiesel production at room temperature. Int. J. Environ. Res. Publ. Health 20, 1760. https://doi.org/10.3390/IJERPH20031760, 2023.